Distributed sensor array for bottom inversion

Sérgio M. Jesus
Larsys, Institute for System and Robotics
University of Algarve, Campus de Gambelas
Faro, 8005–139 Portugal
Email: sjesus@ualg.pt

***Abstract*—Seismic inversion with an AUV-based sensor array system is an appealing concept that opens up a number of interesting possibilities but faces also a number of technological and scientific challenges. Among the technological challenges there is the fact that sensor arrays are no longer hardwired to the tow ship and therefore on the fly data monitoring imposes stringent restrictions on the amount of data that can be sent to the support ship. One of the scientific challenges is to determine the optimal sensor array configuration by exploring AUV mobility for inverting the bottom geophysical structure of interest. In fact, the industry standard planar array and the associated acoustic data processing may not be the setup with the highest performance for each scenario at hand. Generic optimization of sensor distribution through space has been a long standing problem to which there are no closed form solutions. Generically speaking, field diversity maximization is often referred to as a criteria for sensor positioning. This work explores data incoherence as a possible criteria to derive performance of distributed sensor arrays. Additional technological limitations such as array aperture, number of sensors and distances between vehicles impose additional constraints leading to suboptimal configurations. Compressed sensing array processing is used both to explore data incoherence and to offer data reduction for alleviating on the fly monitoring.**

I. Introduction

The energetic transition to renewable sources, namely offshore wind and wave energy platforms, as well as the appetite for rare minerals and other exotic substances impose new operational requirements in geoacoustic challenging environments. A geoacoustic challenging environment has space/time features in terms of water depth variability, spatial changing sub-bottom formations, coastal specific characteristics and environmentally sensitive habitats, that challenge standard surveying apparatus such as those currently used in oil-gas seismic surveying which are based on rigid source-receiver geometries and source firing protocols.

The Widely Scalable Mobile Underwater Sonar Technology (WiMUST) project[1] addresses this challenge by proposing to replace the traditional towed receiving array system by a coordinated fleet of Autonomous Underwater Vehicles (AUVs). The flexibility provided by a receiving fleet of AUVs may address the challenges if fitted with i) the appropriate navigation control for keeping a predetermined formation over long periods of time, ii) wireless communication of data and commands between AUVs and the control and command station and iii) acoustic signal processing to handle on the fly monitoring of the data being acquired and adapt to the complex surveyed environment. This paper focus on the latter challenge and devises new possibilities for on the fly data reduction to be performed on board the vehicles and for determining optimal spatial sensor array distribution for bottom inversion and feature extraction.

There is an extensive literature on ocean bottom estimation by acoustic remote sensing that traces back to the pioneering work of Yilmaz [1], [2], Frisk [3]–[5] and many others. In the last two decades with the advent of fast digital data processors and advanced micro-technology, the scientific community split into two classes of techniques: 1) seismic arrival-based time domain and 2) model or matched-field-based. The former is widely used in the oil-gas seismic industry while the later is concentrated in the academic and scientific community.

Although very general in principle these two approaches, target two different types of environment: low resolution bottom deep targets for the oil-gas industry and high resolution superficial detailed sediments for the scientific community. The WiMUST AUV-based system is meant to be flexible so, in the future, it could encompass one and the other objectives but, at this stage, it will mostly address the second target of high resolution sediments in flexible shallow water, variable bathymetry and complex coastline scenarios [6].

Besides the differences in objectives and target scenarios, all acoustic based bottom inversion techniques boil down to one single but complex problem: how to simultaneously match time-delays, layer thicknesses and sediment velocities to a set of acoustic bottom returns. The relation between these three quantities can be geometrically established in a fairly simple form for some ray paths in given scenarios but, generally, only the time-delays are directly retrieved so one of the two others has to be assumed. This creates a multiple fit problem that may be expressed as a system of equations which entries are related to acoustic wave propagation in the water column and in the bottom, while the bottom itself is unknown. It is therefore a non-linear problem.

The approach proposed in this paper draws its roots in the recent field of compressed sensing, also known as compressive sensing (CS). CS deals with sparse systems of equations where highly dimensional vectors evolve in low-dimension subspaces and can, therefore, according to the CS theory, be sampled at a lower rate than that imposed by Nyquist. CS is attractive for our problem since bottom sediments' discrimination may be modeled as a dense system with often only a few significant reflectors, therefore as a sparse system. This concept was already used on the receiver side [7] and for the source firing system [8]. Another interesting property is that CS deals with random measurements which are likely to occur in WiMUST

[1]WiMUST project, funded by the Horizon 2020 European Research Program under contract number 645141 (see www.wimust.eu for further details).

due to navigation inherent inaccuracies of the fleet of AUVs and clock synchronization issues. Finally, CS techniques are based on l_1 minimization and have therefore low computational requirements, which is an advantage for embarked systems.

This paper is organized as follows: section II describes CS, coherence and diversity based techniques as a potential criteria for distributed array geometry optimization; section III gives the typical simulation scenario and the bottom observation model; section IV describes the simulation and shows the results. Finally, section V gives some conclusions of this work and hints for next steps.

II. CS, COHERENCE AND DIVERSITY

A. CS basics

Let us assume that a signal $\mathbf{s}$ can be written as a finite linear combination of basis vectors $\boldsymbol{\psi}$, such that

$$\mathbf{s} = \sum_{m=1}^{M} x_m \boldsymbol{\psi}_m \tag{1}$$

where x_m are the basis coefficients and M is the number of degrees of freedom. Equation (1) may also be written in a compact matrix form as $\mathbf{s} = \boldsymbol{\Psi}\mathbf{x}$, and where $\boldsymbol{\Psi}^T\boldsymbol{\Psi} = M\mathbf{I}$[2]. Assume now the simple case where the observation $\mathbf{y}$ of $\mathbf{s}$ can be written as

$$\begin{aligned} \mathbf{y} &= \boldsymbol{\Phi}\mathbf{s} \\ &= \mathbf{A}\mathbf{x}, \end{aligned} \tag{2}$$

where $\mathbf{y}$ is $N \times 1$ with $N \ll M$, $\mathbf{A} = \boldsymbol{\Phi}\boldsymbol{\Psi}$, with $\boldsymbol{\Phi}^T\boldsymbol{\Phi} = \mathbf{I}$ and therefore $\mathbf{A}^T\mathbf{A} = M\mathbf{I}$. The objective of the "imaging problem" is, of course, to uniquely determine $\mathbf{x}$ given $\mathbf{y}$ and $\mathbf{A}$, full rank. Since $N \ll M$, the rank of $\mathbf{A}$ is equal to N and the problem is under-determined, so $\mathbf{x}$ can not be uniquely "reconstructed" (using the imaging terminology). There is, however, one way out if $\mathbf{x}$ is sparse, *i.e.*, if the number of its non zero entries $K = \|\mathbf{x}\|_0 \ll M$[3], in which case (1) reduces to K terms with $K \ll N \ll M$. In that case, one solution would be given by

$$\min \|\mathbf{x}\|_0, \qquad \text{s.t.} \qquad \mathbf{y} = \mathbf{A}\mathbf{x} \tag{3}$$

which is infeasible in practice. Instead the problem

$$\min \|\mathbf{x}\|_1, \qquad \text{s.t.} \qquad \mathbf{y} = \mathbf{A}\mathbf{x} \tag{4}$$

may be solved using linear or quadratic optimization techniques. The trick that pushed CS into the scene is the seminal work of Donoho [10] that showed that, under certain conditions on $\mathbf{A}$ and due to the sparsity of $\mathbf{x}$, (3) and (4) have the same and unique solution. The conditions imposed on $\mathbf{A}$ go along two main alternative avenues: isometry or incoherence. Candès [11] has shown that a sufficient condition for Donoho's proof to hold is that $\mathbf{A}$ should verify the Restricted Isometric Property (RIP) (see [11] for a definition) which is shared, for instance, by Gaussian random matrices. Incoherence instead refers to the fact that the inner product of any two different columns of $\mathbf{A}$ should be small, although "small" is not clearly defined. In the next section we attempt to quantify this and take the necessary conclusions of a "small incoherence" matrix $\mathbf{A}$ for CS to work.

[2]this unusual normalization follows that proposed in [9], where $\|\boldsymbol{\psi}_i\| = \sqrt{M}$ contributes to simplification in the sequel.

[3]here, the number of non-zero components is given by the l_0 norm $\|\cdot\|_0$.

B. Coherence and diversity

Coherence plays an important role in physics. In particular the coherence of the underwater acoustic field in time and space allows for information extraction in coherent communications and in array processing (see [12] and [13] for examples). In general a higher coherence allows, when properly exploited, a better performance. In sparse systems such as those mentioned in the previous section, coherence has a counter intuitive role: the smaller the coherence the better.

Mutual coherence is defined as [9]

$$\mu(\mathbf{A}) = \max_{i=1,N;j=1,M} |a_{ij}|, \tag{5}$$

which is directly bounded in $[1, \sqrt{M}]$, *i.e.*, it has the same bounds as the non-normalized plain coherence $C(\mathbf{A})$ given by [14]

$$C(\mathbf{A}) = \max_{\substack{j,k=1,M \\ j\neq k}} \sqrt{\frac{1}{N}|\mathbf{a}_j^T\mathbf{a}_k|}, \tag{6}$$

and bounded in

$$1 \leq C(\mathbf{A}) \leq \sqrt{M}. \tag{7}$$

Of course, having the same bounds does not mean having the same value so, in general, $C(\mathbf{A}) \neq \mu(\mathbf{A})$.

An interesting result mentioned in [9], [15] gives the required number of measurements N for a given sparsity level, bounded by the coherence $\mu(\mathbf{A})$, as

$$N \geq c\mu^2(\mathbf{A})K \log M. \tag{8}$$

where c is some positive constant, and where all other terms have been defined. Interestingly, if the coherence $\mu(\mathbf{A})$ is close to one, $K \log M$ observation samples, instead of M, are sufficient for solving (2), an extraordinary difference for large M. Figure 1 illustrates (8) where the number of samples per resolvable layer (N/cK, for $c = 1$) have been translated into bottom depth using a constant sampling rate of 5 cm[4]. It can

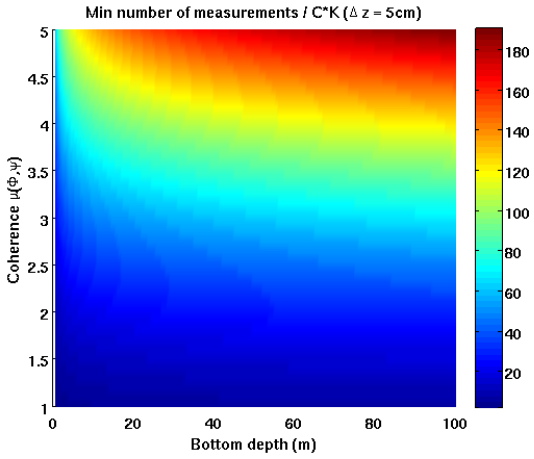

Fig. 1. *Minimum number of required measurement samples per resolvable layer as a function of bottom depth and mutual coherence for a constant and fixed bottom resolution of 5 cm.*

be easily seen that for moderate coherence, say between 1

[4]as an example, a bottom penetration of 50 m requires $M = 50/0.05 = 1000$ samples.

and 2, a low number of 20 to 40 measurements per resolvable layer may be used, almost independently from the required bottom penetration. This is the reason why CS is essentially devoted to low coherence measurements, where the gain is most prominent. It can be shown that the mutual coherence $\mu(\mathbf{A})$ in (8), can be replaced by the non-normalized plain coherence $C(\mathbf{A})$ (6) and the relation still holds.

Relation (8) gives a figure and a more exact meaning to the statement "small coherence" and therefore to the degree of "flatness" required for matrix $\mathbf{A}$. A matrix with high coherence will have high "peaks" and deep "valleys" and will have a low probability to succeed in the inversion of a low K-sparse signal. Conversely, a well distributed matrix with dispersed small values all over its rows and columns, will show a low coherence and therefore a high probability for observing (and then inverting) a low K-sparse signal. A high coherence observation would require that the information is concentrated on a few points, one would say that the **diversity is low**, instead, in a low coherence observation the information is spread out and the **diversity is said to be high**. In other words diversity and coherence are associated and should be the key for determining optimal sensing structures.

III. Simulation scenario and observation model

A. Simulation scenario

Acoustic propagation through the water-bottom interface and then through subsequent interfaces beneath can be accurately handled with the Ocean Acoustics and Seismic Exploration Synthesis (OASES) model [16]. A typical environmental scenario to be used in the simulations is shown in figure 2. The

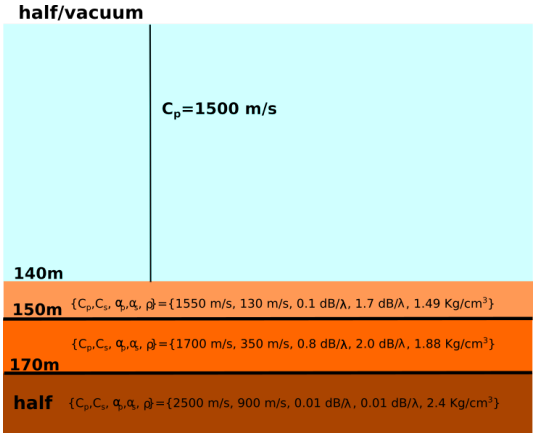

Fig. 2. *Canonical case 1d environmental scenario.*

equipment used for bottom exploration assumes an explosive point source located near the surface at 5 m depth, emitting broadband pulses. The sensing system is a towed horizontal array located at the same depth of the source and at a distance of 200 m for the simulation scenario.

As a first step the OASES transmission loss module (OAST) was used to give a generic overview of the attenuation field over the water column and through bottom layers. This is shown in figure 3 for the frequency of 500 Hz and source depth of 5m. Several obvious remarks can be made: i) at high grazing angles (near vertical) bottom penetration is very

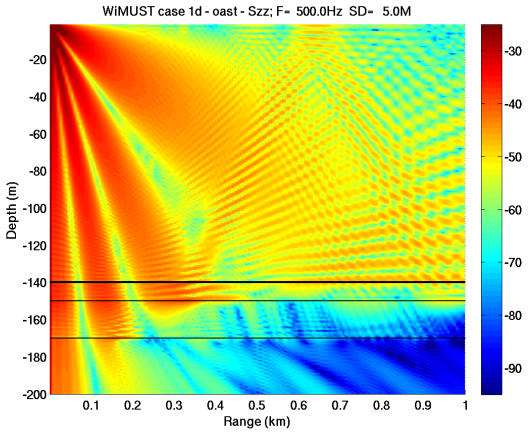

Fig. 3. *Transmission loss for the canonical scenario case 1d of figure 2 at 500 Hz and for a source depth of 5m.*

high and the sound covers all the layers down to the half space; ii) at approximately 100 m range the half space cut-off angle of $\approx 47°$ is reached and beyond that grazing angle the penetration reaches only the second bottom layer, this happens until approximately 250 m range; iii) beyond that range, for a grazing angle of $\approx 24°$, most of the energy reaches only the first sediment layer until $\approx 15°$, at 450 m range, beyond which it almost completely reflects at the water - bottom interface and then bounces back to the surface generating the usual interference pattern with the direct and surface reflected paths; iv) it is interesting to note that for the first and second cutoff angles almost no energy propagates horizontally in the sediments while for the third cutoff angle between 250 and 450 m part of the energy is horizontally transmitted into the sediment, eventually crossing back into the water at longer ranges.

B. Observation model

There are at least two mechanisms for representing the interaction of the acoustic wave with the bottom layers. One is reflection and the other is scattering. Generally speaking it is normally admitted that if the acoustic wave is simply diverted by the density variable layers without particle interaction the wave is said to be reflected; in the opposite, if particle interaction actually occurs resulting in a path change, scattering is said to be at play.

The question posed in this section is whether the sub-bottom layers should be considered as scatterers or as reflectors of the acoustic field. In general reflection is well adapted for the water column that, in the useful frequency range, may be considered as homogeneous and where the compressional sound speed is smoothly variable. Instead, the water - bottom interface can seldom be considered as smooth in practice and the sediment itself is often an inhomogeneous propagation media with upward refracting sound speed gradients due to sediment consolidation and increased density as depth into the bottom increases. In what concerns the bottom, the reflection mechanism can be seen as a simplification of the actual propagation mechanism which is actually closer to scattering.

The received field at observation location ξ_n due to a

unit amplitude monochromatic point source located at ν_s may be written using the Green function $G(\cdot)$, solution of the Helmholtz equation, between two points in space, as

$$G^E(\xi_n, \nu_s) = G(\xi_n, \nu_s) + G^R(\xi_n, \nu_s), \quad n = 1, \ldots, N \quad (9)$$

where

- the sensor array locations (assumed horizontal without loss of generality) are determined by vector $\xi(r, z_r)$ so that $\{\xi_n(r_n, z_r); n = 1, \ldots, N\}$ is called the *sensor domain*,
- the sub-bottom layers are the targets - the *target domain* - for inversion and are designated by position vector $\{\nu_m(r_m, z_m); m = 1, \ldots, M\}$,
- source S is at $r = 0$ and depth z_s, so its position vector is $\nu_s(0, z_s)$ - the *source domain*,
- $G^E(\xi_n, \nu_s)$ is the total excitation field measured at ξ_n due to the source at position ν_s,
- $G(\xi_n, \nu_s)$ represents the incident field received at ξ_n due to a source located at ν_s,
- $G^R(\xi_n, \nu_s)$ is the Green function solution of the wave equation in a stratified media for a source at position ν_s and array sensor at position ξ_n.

so the reflected field is given as

$$G^E(\xi_n, \nu_s) - G(\xi_n, \nu_s) = G^R(\xi_n, \nu_s), \qquad n = 1, \ldots, N \quad (10)$$

The bottom reflected field only, *i.e.*, the field assuming smooth interfaces and perfectly homogeneous propagation media obtained with the pulse option module OASP of the OASES package, in the canonical scenario of figure 2 is shown in figure 4, which is basically the total field minus the direct and surface reflected fields, for various receiver ranges.

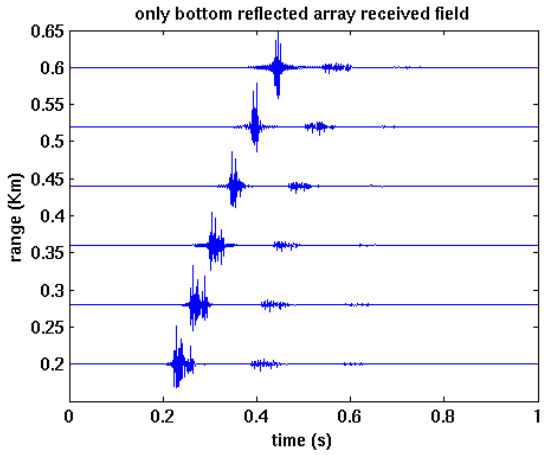

Fig. 4. *OASP calculated bottom reflected field in the band 200-800 Hz for canonical environmental scenario case 1d of figure 2 with source and horizontal receiving array both at 5m depth.*

The monochromatic scattered field observed at location ξ_n for $n = 1, \ldots, N$ receivers, may be written as [14]

$$G^E(\xi_n, \nu_s) = G(\xi_n, \nu_s) + \sum_{k=1}^{K} a_k G^E(\nu_k, \nu_s) G(\xi_n, \nu_k), \quad (11)$$

where

- a_k is the complex amplitude coefficient of the k-th scatterer assumed random distributed,
- K is the number of effective scatterers,
- $G^E(\nu_k, \nu_s)$ is the excitation field of k-th scatterer located at ν_k due to the source at position ν_s,
- $G(\xi_n, \nu_k)$ is the Green function between scatterer at position ν_k and array sensor at position ξ_n.

and where all the other quantities have been previously defined. Effectively, the k-th scatterer excitation field $G^E(\nu_k, \nu_s)$ should encompass not only the source incident field but also the field due to all the other $K - 1$ scatterers. In that setting the problem becomes nonlinear and requires the inversion of the inter-scatterer excitation matrix for determining the actual excitation at each scatterer, the so-called Foldy-Lax system (see details in [17]). Approximating the excitation field $G^E(\nu_k, \nu_s)$ by the incident field $G(\nu_k, \nu_s)$, known as the Born approximation, is widely used in various fields such as in radar imaging and optics. The great advantage of the Born approximation is to allow for problem linearization and thus to write the bottom scattered field at receivers $n = 1, \ldots, N$ as

$$G^E(\xi_n, \nu_s) - G(\xi_n, \nu_s) = \sum_{k=1}^{K} a_k G(\nu_k, \nu_s) G(\xi_n, \nu_k). \quad (12)$$

Equation (12) was used to compute the bottom scattered field assuming that the bottom can be represented by an ensemble of point virtual sources excited with the bottom incident field due to the explosive water column point source. These are the $M = 5000$ point scatterers distributed along a vertical grid of 100×50 points in depth and range, respectively. The aperture is 60 m in depth (into the bottom) and for the canonical example 700 m in range. This range covers the distance between the acoustic source and the whole horizontal array aperture.

The result obtained with OASP propagation model for a 200-800 Hz bandwidth, is shown in figure 5: for the bottom received pulses at zero range (a) and for the horizontal array receivers at various ranges (b). Both source and horizontal array are at 5m depth. One can note the resemblance of the scattered field with the overall time arrival structure of the bottom reflected field with, however, a few more scatterers leading to a several low amplitude late arrivals.

IV. CS BOTTOM INVERSION RESULTS

The array received field was simulated using OASP at a single monochromatic frequency of 500 Hz. A bottom grid of 50×10 (M=500) points for 60×2500m was selected to scatter the array acoustic source received signal and received in a N =100 sensor array with 2.5 km aperture. A signal-to-noise ratio (SNR) of 10 dB was used. The environmental scenario is that of Fig. 2. A number of K=30 bottom scatterers were simulated at variable bottom depths placed along equispaced range intervals according to (12) and decreasing values of a_k with depth. So, vector $\mathbf{x}$ has dimension $M = 500$ with $K = 30$ values different from zero. Channel matrix $\mathbf{\Psi}$

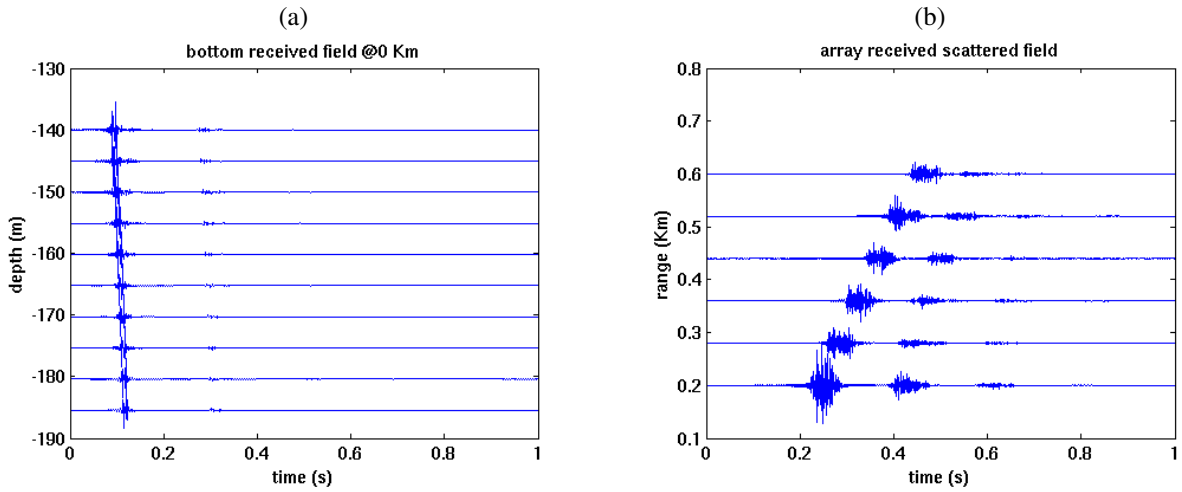

Fig. 5. *Bottom scattered field computed with OASP in the environmental scenario case 1d of figure 2: bottom incident field, term $G(\nu_k, \nu_s)$ at source range (a) and horizontal receiving array bottom scattered field at depth 5 m and various ranges using (12) (b).*

contains the Green functions, solutions of the wave equation and observation matrix $\mathbf{\Phi}$ selects $N = 100$ observation sensors at random (uniformly distributed) positions along the line array at 5m depth (equal to source depth). This random selection allows to obtain a low coherence of $\mu(\mathbf{A}) = 1.3$ (see figure 1 and associated discussion about coherence).

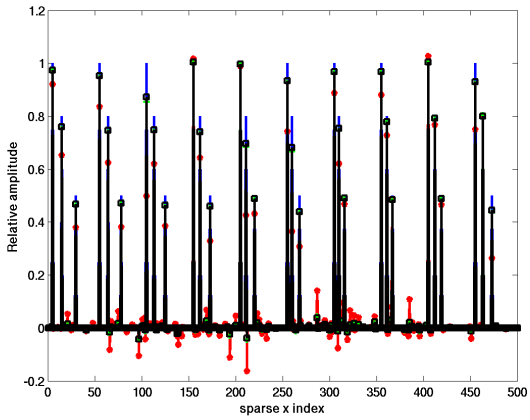

Fig. 6. *sparse vector* $\mathbf{x}$ *amplitude estimate at 500 Hz: true values (solid blue), Basis Pursuit (red asterisks), L1/L2 (green +) and L1/L2 constrained (solid black squares).*

Three algorithms from the YALL package[5] were used: the Basis Pursuit minimum l_0 (BP), the l_1 norm l_2 unconstrained (L1/L2) and the l_1 minimization - l_2 constrained (L1/L2c). The CS inversion results are shown in figure 6 for vector $\mathbf{x}$: true values (solid blue), BP (red asterisks), L1/L2 (green +) and L1/L2c (black squares). It is clear that the estimated closely follows the true values with however a few amplitude errors that are higher at greater depths (lower amplitudes) and a few background clutter that is higher for the BP estimate (red *). Figure 7 shows the reconstructed bottom reflecting field associated with the L1/L2 constrained estimate which provides the lowest estimation error. This result is due to the

[5]from Yin Zhang, Junfeng Yang and Wotao Yin, Rice University, `yall1.blogs.rice.edu`.

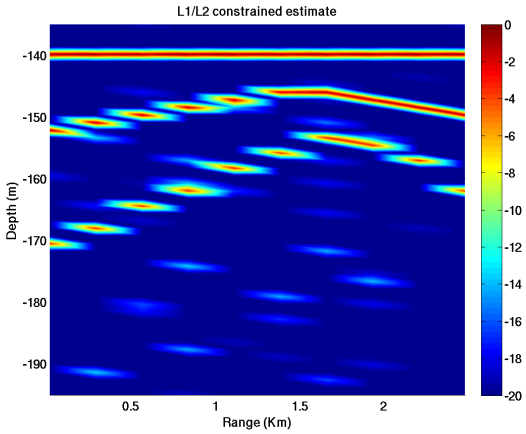

Fig. 7. *bottom localized reflector estimates using the L1/L2 constrained algorithm at 500 Hz.*

better handling of the observation noise through the norm 1 minimization and square error constrained such as (see YALL package documentation for details)

$$\min_{\mathbf{x}} \|\mathbf{x}\|_1, \quad \text{s.t.} \quad \|\mathbf{Ax} - \mathbf{y}\|_2 \leq \delta \tag{13}$$

where δ is some positive constant.

V. Conclusion and Perspectives

This paper presents a preliminary assessment on the usage of CS techniques for geoacoustic inversion in the context of the WiMUST project scenario. This scenario encompasses a sensor array formed by a series of free to move small arrays towed by AUV's along predetermined paths, effectively forming a distributed sensor array. One of the questions associated with this distributed sensor array is where should its sensors be located for optimal solution of the problem at hand of determining bottom properties. It appears clear from the results that low observation coherence plays an important role in the optimal sampling of the bottom return field. This low

coherence requirement may be viewed as a quest for higher diversity and therefore a richer observation.

CS inversion of bottom returns of a monochromatic wave at 500 Hz in a simulated environment show the potential of the technique for a mismatch free benign bottom and an SNR of 10 dB. Further study is necessary for testing the array distribution criteria for 2D and 3D arrays as well as its behavior relative to broadband signals and various practical constraints on limitations imposed by AUV navigation for keeping close formations during long periods of time. Bottom inversion testing in mismatch situations and in more challenging environments is also necessary.

ACKNOWLEDGMENT

This work has received funding from the European Union's Horizon 2020 research and innovation program under grant agreement No. 645141 (WiMUST project)

REFERENCES

[1] O. Yilmaz and J. Claerbout, "Pre-stack partial migration," *Geophysics*, vol. 45, no. 12, pp. 1753–1779, 1980.

[2] O. Yilmaz, *Seismic data processing*. Tulsa: SEG, 1987.

[3] G. Frisk and J. Lynch, "Shallow water waveguide characterization usign the hankel transform," *J. Acoust. Soc. America*, vol. 76, pp. 205–216, 1984.

[4] G. Frisk, J. Lynch, and J. Doutt, "The determination of geoacoustic models in shallow water," in *Ocean Seismo-Acoustics*, T. Akal and J. Berkson, Eds., Plenum, New York, 1986, pp. 998–1017.

[5] G. Frisk, J. Lynch, and S. Rajan, "Determination of compressional wave speed profiles using modal inverse techniques in a range-dependent environment in nantucket sound," *J. Acoust. Soc. America*, vol. 86, no. (2), pp. 1928–1939, November 1989. [Online]. Available: http://dx.doi.org/10.1121/1.398571

[6] H. Al-Khatib, G. Antonelli, A. Caffaz, A. Caiti, I. B. d. J. G. Casalino, H. Duarte, G. Indiveri, S. Jesus, K. Kebkkal, A. Pascoal, and D. Polani, "The widely scalable mobile underwater sonar technology (wimust) project: an overview," in *MTS/IEEE Oceans'15*, Genova, Italy, 2015.

[7] C. Yardim, P. Gerstoft, W. Hodgkiss, and J. Traer, "Compressive geoacoustic inversion using ambient noise," *J. Acoust. Soc. America*, vol. 135, no. 3, pp. 1245–1255, March 2014. [Online]. Available: http://dx.doi.org/10.1121/1.4864792

[8] F. Herrmann, "Sub-nyquist sampling and sparsity: how to get more information from fewer samples," in *Proc. Soc. Exploration Geophysicists Annual Meeting*, Houston, US, October 2009, pp. 3410–3415.

[9] E. Candès and J. Romberg, "Sparsity and inchoerence in compressive sampling," *Inverse Problems*, vol. 23, pp. 969–985, 2007.

[10] D. Donoho, "Compressed sensing," *IEEE Trans. Inform. Theory*, vol. 52, no. 12, pp. 5406–5425, December 2006.

[11] E. Candès, J. Romberg, and T. Rao, "Robust uncertainty principles: exact signal reconstruction from highly incomplete frequency information," *IEEE Trans. Inform. Theory*, vol. 52, no. 2, pp. 489–509, February 2006.

[12] U. Vilaipornsawai, A. Silva, and S. Jesus, "Experimental testing of asymmetric underwater acoustic networks," in *Proc. of Int. Conf. Communications and Electronics ICCE 2014*, Da Nang, Vietnam, July 2014.

[13] H. Krim and M. Viberg, "Two decades of array signal processing research," *IEEE Signal Processing Magazine*, vol. 96, pp. 67–94, July 1996.

[14] A. Fannjiang, P. Yann, and T. Strohmer, "Compressed remote sensing of sparse objects," *arXiv:0904-3994*, 2009.

[15] E. Candès and M. Wakin, "An introduction to compressive sampling," *IEEE Signal Processing Magazine*, vol. 25, no. 3, pp. 21–30, March 2008.

[16] H. Schmidt, *OASES 3.1 - User guide and reference manual*, MIT, March 2011.

[17] K. Huang, K. Solna, and H. Zhao, "Generalized Foldy-Lax formulation," *J. Comput. Physics*, vol. 229, pp. 4544–4553, 2010.